Bone marrow mesenchymal stem cell-derived exosomes loaded with miR-26a through the novel immunomodulatory peptide DP7-C can promote osteogenesis

Shuang Lai (laishaung1109@gmail.com)
University of Electronic Science and Technology of China https://orcid.org/0000-0001-8765-0484
Li Deng
University of Electronic Science and Technology of China
Cong Liu
University of Electronic Science and Technology of China
Xinlun Li
Southwest Medical University
Liyuan Fan
University of Electronic Science and Technology of China
Yushu Zhu
Southwest Medical University
Yiling Yang
Southwest Medical University
Yandong Mu
University of Electronic Science and Technology of China Sichuan Provincial People's Hospital: Sichuan Academy of Medical Sciences and Sichuan People's Hospital https://orcid.org/0000-0002-1829-6116

Research Article

Keywords: Exosomes, miR-26a, osteogenesis, DP7-C

Posted Date: October 4th, 2022

DOI: https://doi.org/10.21203/rs.3.rs-2037065/v1

Version of Record: A version of this preprint was published at Biotechnology Letters on May 17th, 2023. See the published version at https://doi.org/10.1007/s10529-023-03376-w.

Abstract

Purpose: As small bioactive molecules, exosomes can deliver osteogenesis-related miRNAs to target cells and promote osteogenesis. This study aimed to investigate miR-26a as a therapeutic cargo to be loaded into exosomes through a novel immunomodulatory peptide (DP7-C). In addition, the exosomes secreted from BMSCs were obtained to evaluate their osteogenic capacity.

Methods: After transfecting BMSCs with DP7-C as a transfection agent, exosomes were extracted by ultracentrifugation from the culture supernatant of miR-26a-modified BMSCs. Then, we characterized and identified the engineered exosomes. Next, the effect of the engineered exosomes on osteogenesis was evaluated in vitro and *in vivo*, including in Transwell, wound healing, modified Alizarin red staining, western blot, real-time quantitative PCR, and experimental periodontitis assays. Finally, bioinformatics and data analysis were used to investigate the role of miR-26a in bone regeneration.

Results: The DP7-C/miR-26a complex successfully transfected miR-26a into BMSCs and stimulated them to release a high dosage of exosomes overexpressing miR-26a. Furthermore, exosomes loaded with miR-26a could promote the proliferation, migration, and osteogenic differentiation of BMSCs in vitro and inhibit the destruction of periodontitis *in vivo*, maintaining the integrity of supporting periodontal tissue. Target gene analysis indicated that the osteogenic effect of miR-26a is related to the mTOR pathway.

Conclusion: MiR-26a can be encapsulated into exosomes through DP7-C. Exosomes loaded with miR-26a can promote osteogenesis and inhibit bone loss in experimental periodontitis and serve as the foundation for a novel treatment strategy.

Introduction

Oral inflammation, trauma, tumors, and deformities are the leading causes of bone fracture, which seriously affects patients' quality of life. Osteoinduction via the implantation of biomaterials is the core technology of current clinical treatment. However, the treatment above has serious risks, such as transplant rejection and infection. In recent years, using acellular scaffolds for bone tissue regeneration has become a very promising strategy for bone tissue repair.

Exosomes are microscopic, secreted membrane particles of 30–150 nm that can serve as extracellular communication vehicles, transporting bioactive proteins, nucleic acids, and lipids among cells to induce biological reactions in targeted cells(Kalluri & LeBleu, 2020; M.Liu; Y.Sun, 2018; Roberts, Langer, & Wood, 2020). As an essential mediator of intercellular transport and communication, exosomes are also a "natural nanoscale transport material" that can be loaded with miRNAs or cytokines(Thakur, Parra, Motallebnejad, Brocchi, & Chen, 2022). With the development of "cell-free therapy," the application of exosomes in bone tissue engineering has attracted increasing attention. Numerous studies have proven that exosomes from bone marrow mesenchymal stem cells (BMSCs) have pro-osteogenic effects(Z. Y. Li et al., 2022). In addition, as short noncoding single-stranded endogenous RNAs that range in length from

20 to 24 nucleotides, miRNAs have long been recognized for their role in promoting osteogenesis(Lanzillotti et al., 2021).

As biologically active small molecules, exosomes have become effective carriers for the delivery of miRNAs. Based on our previous research, DP7-C is a cationic antimicrobial peptide that was simulated by a computer. It has immune regulation and delivery carrier functions(Zhang et al., 2020; Zhang et al., 2021). As a conveyance vector, DP7-C has more benefits in terms of transfection effectiveness and cytotoxicity than the commercial transfection reagent. However, there is no research on cell-derived exosomes after transfection with DP7-C. In this study, we utilized DP7-C to deliver microRNAs.

Based on the above, we envisage using exosomes for the delivery of osteopromoting miRNAs. We innovatively used the complex of DP7-C and miR-26a to transfect bone marrow mesenchymal stem cells to reduce cytotoxicity. By detecting the osteogenic effect of exosomes *in vivo* and in vitro, bioinformatics analysis was carried out, with the aim of providing a specific foundation for future bone regeneration research.

Materials And Methods

Cell isolation and identification

Separate bone marrow mesenchymal stem cells (BMSCs) were obtained from Sprague–Dawley rats (8 weeks, 210 g-230 g, Dassy Experimental Animals, China) via a modified whole bone marrow adherence method. This study was authorized and supervised by the Committee of Sichuan Provincial People's Hospital (Approval No. 20200133). Cells were cultured at 37°C in a 5% CO_2 environment in complete medium, which was DMEM with 10% fetal bovine serum (FBS VWR) and 1% penicillin–streptomycin (PS HyClone). Flow cytometry was used to detect the cellular expression of MSC surface markers (CD29, CD90, CD44, and CD45). We collected 3–5 generations for future experiments.

DP7-C/miR-26a complex transfection into BMSCs

This study utilized passages 3–5 of BMSCs for exosome isolation. Our previous study used computer simulation to create DP7-C, a cholesterol-modified novel cationic and hydrophilic antimicrobial peptide. MiR-26a mimics (UUCAGUAAUCCAGGAUAGGCU) and negative control NC (synthesized by Tsingke Biotechnology) were transfected into BMSCs with DP7-C. In detail, BMSCs (2 X 107 cells) were seeded in a 10 cm plate for 24 h. Then, DP7-C (165 μg) and miR-26a (33 μg) were combined at a ratio of 5:1 (w/w) into DMEM and incubated on ice for 15 min. Finally, the complex was slowly and evenly added into the plates, and cultivation was continued.

Isolation and purification of exosomes derived from BMSCs

After transfection, the culture medium was replaced with exosome-free medium, which was DMEM with 10% exosome-depleted FBS from SBI (System Biosciences, CA, USA) and 1% penicillin–streptomycin (PS HyClone). Forty-eight hours later, the supernatant was collected to obtain and purify exosomes by

ultracentrifugation. Specifically, the supernatants were filtered through a 0.22 m filter after centrifugation at 10,000 × g for 30 min at 4°C to remove cell debris and then centrifuged at 100,000 g with an ultracentrifuge (Optima XPN-100 BECKMAN, USA) for 70 min at 4°C to separate the exosomes. Finally, the exosomes were resuspended in PBS (pH 7.2–7.4, Solarbio, P1020) for further study.

Exosome internalization

Following the manufacturer's protocol, the exosomes were labeled with PKH67 (Umibio, UR52303), a green fluorescent membrane-labeling dye DiI. Next, BMSCs were incubated for 6, 12, 24, and 48 hours with DiI-labeled exosomes. BMSCs were fixed in 4% paraformaldehyde (Solarbio, P110), and then 5 μg/mL phalloidin (Solarbio, CA1670) was used to stain the cytoskeleton, and 5 μg/mL 4',6-diamidino-2-phenylindole dihydrochloride (DAPI, Solarbio, D8200) was used to label the nucleus. The uptake of exosomes by BMSCs was observed via confocal laser-scanning microscopy (ZEISS, Germany).

Cell-Counting Kit-8 assay

BMSCs were trypsinized, counted, adjusted to a density of 1 × 104 cells/mL, seeded in 96-well culture plates and treated with the corresponding interventions. Cell Counting Kit-8 (CCK8, Solarbio, CA1210) was used to evaluate cell proliferation every 24 h. The absorbance value at 450 nm was read by a microplate reader and plotted for the cell growth curve.

Wound healing assay

After the BMSCs reached 90% confluence, they were serum starved for 24 h. The cells were scraped off with the tip of a 10 μL sterile pipette, and a parallel wound was created. The cells were washed three times with PBS to eliminate cell debris. The cell culture wells were divided into blank (PBS), Exo^{NC}, and $Exo^{miR-26a}$ groups. Then, 50 μg/mL Exo^{NC} and $Exo^{miR-26a}$ were added to the groups. After 24 h and 48 h, images were captured with a microscope. The percentage of wound closure was quantified by ImageJ.

Transwell migration assay

BMSCs (5×10^4 cells) were seeded in the upper chambers of Transwell plates (8 μm pores, Corning), and the complete culture medium was placed in the lower chamber as a chemoattractant. Each group was treated with the corresponding interventions. Twenty-four hours later, the cells were stained with crystal violet (Solarbio, C8470). Then, the cells were observed under a light microscope (ZEISS, Germany). ImageJ was used to perform quantitative cell analysis.

ALP activity detection

BMSCs were seeded in 6-well culture plates. The medium was replaced by osteogenic induction medium (DMEM with 10% FBS, 1% penicillin–streptomycin, 20 mmol/L β-glycerophosphate, 50 g/mL vitamin C and 10 mol/L dexamethasone). Next, the blank (PBS), Exo^{NC}, and $Exo^{miR-26a}$ suspensions were added to the cells at 50 μg/mL, and the medium was replaced every 3 days. After 7 days of osteogenesis induction, an ALP activity assay kit (Beyotime, China) was used to assess alkaline phosphatase activity. The BMSCs were harvested and then lysed with cell lysis buffer. The supernatant was collected after

centrifugation at 10,000 × g for 5 min at 4°C, and the ALP activity was measured according to the manufacturer's instructions.

Alizarin red staining

After 21 days of osteogenesis induction, the BMSCs were fixed with 4% paraformaldehyde on ice for 30 min and then dyed with Alizarin Red S Staining Solution (Solarbio, G3280) for 3 min. After washing 3 times with PBS, the calcified nodules of bone marrow mesenchymal stem cells were observed by light microscopy (ZEISS, Germany) and photographed.

Western blotting

Exosomes and cells were collected and lysed in cell lysis buffer (Solarbio, R0100). SDS—PAGE was used to isolate the proteins. Western blotting primary antibodies used included antibodies against GAPDH (1:20000 dilution, Huabio, China), CD63 (1:1000 dilution, Abcam, UK), CD81 (1:1000 dilution, Abcam, UK), TSG101 (1:1000 dilution, Abcam, UK), Calnexin (1:1000 dilution, Abcam, UK), ALP (1:4000 dilution, Huabio, China), BMP2 (1:1000 dilution, Huabio, China), RUNX2 (1:500 dilution, Huabio, China), and COLIA1 (1:1000 dilution, Huabio, China), and an HRP-conjugated goat anti-rabbit/mouse secondary antibody (1:5000 dilution, Huabio, China) was used. The bands were then visualized using a Super ECL kit (Solarbio, PE0010). Tanon-5200 was used for exposure.

Real-time quantitative PCR (RT—qPCR)

Following total RNA extraction from cell samples with TRIzol™ Reagent (Invitrogen, USA), the RNA was used to synthesize cDNA with M-MLV (Thermo Fisher Scientific). The cDNA was then used as a template for PCR using the diverse primers listed in Table 1 (designed and synthesized by Tsingke, China), and the 7500 Real-Time PCR System was used to assess the level of mRNA expression. The average threshold cycle (Ct) for each gene was determined from triplicate reactions. Using the $2 - \Delta\Delta Ct$ method, the relative expression level of mRNA or miRNAs was standardized to that of the internal controls GAPDH or U6.

Table 1
The primers for qRT-PCR

Gene name	Primers
ALP	Forward: 5′-CTTGAAGTGTTGCATGGGC-3′
	Revise: 5′-CAAGTCTCAGGGTGGAAAGG-3′
COL1A1	Forward: 5′-CCCCTGGAAAGAATGGAGATG-3′
	Revise: 5′-TCCAAACCACTGAAACCTCTG-3′
RUNX2	Forward: 5′-CCCAGTATGAGAGTAGGTGTCC-3′
	Revise: 5′-CGCCTGGGTCTCTTCACTAC-3′
BMP2	Forward: 5′-GGGTAAGACTGGTCATAGGACC-3′
	Revise: 5′-GCTTGGACATGAAGGCTTTG-3′
miR-26a	Forward: 5′-UUCAAGUAAUCCAGGAUAGGCU-3′
	Revise: 5′-CCUAUCCUGGAUUACUUGAAUU-3′
NC	Forward:5′-UUCUCCGAACGUGUCACGUTT-3′
	Revise:5′-ACGUGACACGUUCGGAGAATT-3′
U6	Forward:5′-AGCACATATACTAAAATTGGAACGAT-3′
	Revise: 5′-ACTGCAGGGTCCGAGGTATT-3′
GAPDH	Forward: 5′-CCACCCATGGCAAATTCCATGGCA-3′
	Revise: 5′-TCTAGACGGCAGGTCAGGTCCACC-3′

Animal experiments

After 3 days of environmental acclimation, 18 male C57BL/6 mice (8 weeks, 20–25 g) were randomly divided into the following groups: blank (PBS), Exo^{NC}, and $Exo^{miR-26a}$; each group included 6 mice. According to previous research(Chipashvili & Bor, 2022), a 5 − 0 silk ligature was tied around the left maxillary second molar and tightened to induce experimental periodontitis. After three days of induction, 10 μL of exosome suspension was injected into the palatal gingiva. The injection was repeated every three days until the eleventh day. All the mice were sacrificed for the subsequent evaluations. Microcomputed tomography (μCT, ZEISS) was used to measure bone formation, as well as bone volume/total volume (BV/TV), bone mineral density (BMD), and distance from the CEJ to the AB. Following dehydration, the samples were decalcified in 10% EDTA (pH 7.4) for 14 days before being embedded in paraffin. Five-millimeter sections were cut and prepared for hematoxylin and eosin (HE) staining to evaluate alveolar bone loss.

Bioinformatic analysis of miR-26a target genes

To reduce the false-positive rate, TargetScan, miRmap, PicTar, miRanda, and DIANA-microT were used to predict miR-26a target genes. To investigate the functional evaluation and pathway enrichment of those predicted genes, the HiPlot online analysis tool was used with P0.05 as the significance threshold to obtain important gene sets from the Gene Ontology (GO) and Kyoto Encyclopedia of Genes and Genomes (KEGG) databases.

Statistical analysis

GraphPad Prism 8 was used to analyze the results. The results of three separate experiments are shown as the average standard deviation (SD). The independent two-tailed Student's t test was used to compare the two groups. A two-tailed P value of < 0.05 was regarded as statistically significant.

Results

1. DP7-C efficiently delivers miR-26a into BMSCs.

In previous research, we developed a novel cholesterol-modified cationic and hydrophilic antimicrobial peptide (DP7-C) that can efficiently deliver microRNAs into tumor cells via the DP7-C/miRNA complex (Zhang et al., 2020). To reveal whether the complex can also successfully transfect BMSCs, we first separated bone marrow stromal cells (BMSCs) from rats and identified them by flow cytometry. The double-staining marker set CD90/CD29 was expressed at a high level (96.38%), as was CD44 (96.97%), while the negative marker CD45 was expressed at a low level (1.32%) (Fig. 1A). Then, we compared the cytotoxicity between DP7-C and the commercial transfection agent Lipo 2000 via a CCK8 assay. The BMSC survival curve of DP7-C was flatter than that of Lipo 2000 as time increased, indicating that DP7-C was safer than Lipo 2000 (Fig. 1B). Finally, we obtained extremely high expression of miR-26a in BMSCs by qRT—PCR. For normalization, U6 was utilized (Fig. 1C). Above all, DP7-C can be employed as an effective transfection agent to deliver miR-26a into BMSCs while causing little cytotoxicity.

2. Isolation and characterization of exosomes derived from miR-26a-modified BMSCs.

After successfully transfecting BMSCs with the DP7-C/miR-26a complex, we separated the exosomes from the supernatant and then characterized them. Representative transmission electron microscopy (TEM) images of exosomes isolated from NC BMSCs and miR-26a-modified BMSCs showed no morphological heterogeneity, with a cup-shaped structure (Fig. 2A). Nanoparticle tracking analysis (NTA) indicated that the average particle size of each group was 79.05 nm and 79.11 nm. The difference was not statistically significant (P > 0.05) (Fig. 2B). To observe the uptake of exosomes by BMSCs, PKH67-labeled exosomes (green fluorescence) were added to BMSCs, and the nuclei of BMSCs were stained with DAPI (blue fluorescence). The cytoskeleton was labeled with phalloidin (red fluorescence). As shown in Fig. 2F, the uptake of exosomes was observed at 6, 12, 24, and 48 hours. Furthermore, western blotting validated the presence of the exosomal markers CD63, CD81, and TSG101, while the marker calnexin was

barely detectable marker (Fig. 2C). To detect the additional active loading of miR-26a, we examined miR-26 expression in exosomes by qRT—PCR. The results showed that the expression of miR-26a in the $Exo^{miR-26a}$ group was significantly higher than that in the Exo^{NC} group (Fig. 2D), indicating that we successfully encapsulated miR-26a into exosomes secreted from BMSCs. The concentrations of exosomes stimulated by DP7-c were higher than those of the Lipo 2000 groups (Fig. 2E).

3. $Exo^{miR-26a}$ can improve the migration and proliferation of BMSCs.

The CCK8 assay showed that the $Exo^{miR-26a}$ group showed significantly improved proliferation of BMSCs (Fig. 3A). BMSC migration is the first step of bone development(Su et al., 2018). BMSC migration and differentiation are two critical physiological processes in bone regeneration("NGF-p75 signaling coordinates skeletal cell migration during bone repair,"). Two separate assays were performed to investigate cell migration and motility: the in vitro scratch assay and the Transwell migration assay, which evaluates cell migration and the appearance of intact cell—cell interactions and hence mimics cell migration *in vivo*. As shown in Figs. 3B and C, the $Exo^{miR-26a}$ group showed improved migration of BMSCs cultured for 24 h in Transwell chambers, as shown in the cell number histogram. In the scratch assay, compared to ExoNC, ExomiR-26a demonstrated better cell motility and an increased area covered by the cells (Figs. 3D and E).

4. $Exo^{miR-26a}$ can promote osteogenic differentiation of BMSCs.

To further uncover the osteogenesis ability of $Exo^{miR-26a}$, osteogenic medium was used to induce BMSC osteogenic differentiation. ALP staining and activity in BMSCs treated with $Exo^{miR-26a}$ were considerably higher than those in BMSCs treated with Exo^{NC} (Figs. 4C and E). Alizarin Red S staining consistently showed that osteogenic nodules were significantly increased in the $Exo^{miR-26a}$ group compared with the Exo^{NC} and blank groups (Fig. 4F). Furthermore, qPCR results indicated that the mRNA expression of osteogenesis-related genes such as ALP, BMP2, RUNX2, and COL1A1 was upregulated in the $Exo^{miR-26a}$ group (Fig. 5D). Western blot analysis detected the same trend in protein levels (Figs. 5A and B).

5. $Exo^{miR-26a}$ enhanced bone regeneration in vivo.

An experimental periodontitis model was induced further to investigate the biological role of $Exo^{miR-26a}$ in bone regeneration. The whole experimental design is shown in Fig. 5A. Previous studies have demonstrated that local injection in the gingiva contributes to the enrichment of exosomes(Elashiry et al., 2020). Based on this, after repeated injection of exosomes every three days, the whole maxilla was

surgically removed for subsequent evaluation. 3D reconstruction revealed that the bone regeneration in the $Exo^{miR-26a}$ group was significantly more extensive than that in the Exo^{NC} group (Fig. 5C). The proportion of BV/TV and BMD was significantly increased with $Exo^{miR-26a}$ treatment, according to micro-CT image quantification (Fig. 5B). Correspondingly, the histological sections corroborated the observed bone modifications (Fig. 5D).

6. miR-26a target gene prediction and pathway analysis.

To identify promising miR-26a target genes in BMSC osteogenesis using bioinformatics, the number of target genes of miR-26a was determined to be 2215, 1576, 1089, 749, and 930 based on analysis using DIANA-micro, miRanda, miRmap, PicTar, and TargetScan, respectively. A total of 139 overlapping target genes were included in the bioinformatics analysis (Fig. 6A). Then, Gene Ontology (GO) and Kyoto Encyclopedia of Genes and Genomes (KEGG) were used to explore the mechanisms of miR-26a(Wang et al., 2021; Zeng, Liang, Lan, Zhu, & Liang, 2018). GO biological process analysis revealed that most of the identified target genes were enriched in protein autophosphorylation, peptidyl-threonine phosphorylation, and peptidyl-threonine modification. The identified target genes for the cellular component were closely associated with cytoplasmic stress granules and cytoplasmic ribonucleoprotein granules. The three most enriched molecular functions were ribonucleoprotein complex binding, translation regulator activity, nucleic acid binding, and translation factor activity (Fig. 6B). KEGG enrichment analysis showed that miR-26a could exert significant effects on BMSCs through multiple pathways, including the mTOR signaling pathway and autophagy, as well as the Wnt signaling pathway (Fig. 6C).

Discussion

In the skeleton system, miRNAs have emerged as significant regulators of osteogenic signaling pathways, osteoblast proliferation and differentiation, and bone homeostasis(Lian et al., 2012). Our previous study discovered that miRNAs were differentially expressed in hPMSCs cocultured with HAG during osteogenic differentiation(Deng et al., 2022). Among these miRNAs, miR26-a was significantly overexpressed. Therefore, we focused on miR-26a. Furthermore, recent studies have demonstrated that miR-26a can modulate osteogenic regulation by targeting a variety of miRNAs and proteins. For instance, Li and colleagues discovered that augmenting miR-26a expression *in vivo* in a targeted and sustained manner resulted in complete healing of critical-size calvarial bone fractures and improved vascularization(Y. Li et al., 2013). Other researchers found that miR-26a might serve as a viable therapeutic option for osteoporosis therapy by increasing bone production and promoting osteogenesis during bone fracture repair(Y. Li et al., 2015).

Nanosized vectors are used in regenerative medicine to efficiently deliver a payload to specific target sites(Peng, Chen, & Leong, 2015). Importantly, miRNA medicines require delivery vehicles due to their instability. Exosomes are an excellent choice. Exosomes, as nanoparticles, may retain biological activity for extended periods due to their high natural affinity and extended metabolic half-life. Numerous studies

have revealed that exosomes can stimulate osteogenic differentiation due to increased osteogenic miRNAs, which activate at least two osteogenic differentiation pathways (PI3K/Akt and MAPK)(Fan et al., 2020; Huang et al., 2020; A. Liu et al., 2021; L. Liu et al., 2019; Zhai, Zhu, Yang, & Mao, 2020). Therefore, we envisaged using exosomes as transport vehicles to deliver easily degradable miRNAs.

Loading bioactive substances into exosomes is still a challenging research topic(Jin, Ren, & Qi, 2020; Xu et al., 2020). The two main strategies are electroporation and genetic modification(Vader, Mol, Pasterkamp, & Schiffelers, 2016). This study innovatively used a novel immunomodulatory peptide (DP7-C) to transfect BMSCs without cytotoxicity. The results showed successful loading of miR-26a into BMSCs after incubation with the DP7-C/miR26a complex. One of the drawbacks of cell-free therapy is the difficulty of obtaining large quantities of exosomes(W. Li et al., 2018; Zuo et al., 2019). We discovered that DP7-C could stimulate BMSCs to secrete higher numbers of exosomes than the commercial transfection reagent Lipo 2000 during the process of carrying nucleic acids into cells. As the experiment progressed, we were pleasantly surprised to find that after transfection, BMSCs produced exosomes loaded with miR-26a, which were shown to stimulate BMSC osteogenic development via several parameters. Correspondingly, we established an experimental periodontitis model further to confirm the osteogenic function of exosomes in vivo. The results of microCT and HE staining revealed that $Exo^{miR-26a}$ could attenuate bone loss.

Furthermore, little progress has been achieved in identifying the molecular processes of exosomes loaded with miRNA-26a in BMSCs. As a result, after assessing the osteogenic regulatory role of exosomes carrying miR-26a, we performed a bioinformatics study of the underlying molecular mechanisms to identify miR-26a target genes and signaling pathways. The DIANA-microT, miRanda, miRmap, PicTar, and TargetScan databases were used to analyze the target genes of miR-26a, and 139 target genes were obtained after intersection analysis(Pian, Zhang, Gao, Fan, & Li, 2020). Following comprehensive target gene network analysis, GO enrichment analysis revealed that miR-26a target genes were considerably enriched in protein autophosphorylation and cell proliferation. According to our KEGG pathway analysis, miRNA-26a may play a pivotal role in BMSC osteogenesis via numerous pathways, including the mTOR signaling pathway related to bone regeneration. The mTOR signaling pathway transmits and integrates several signals, such as those related to growth factors, nutrition, and energy metabolism. These signals have been reported to function in musculoskeletal development(Dai et al., 2017).

However, there are certain limitations to this study that should be mentioned. The results of bioinformatics analysis were not verified through experimentation. Our findings will need to be confirmed shortly by utilizing both in vitro and *in vivo* clinical and molecular biological techniques. Thus, we intend to investigate the target genes and particular signaling pathways that exosomes laden with miR-26a use to modulate the osteogenic differentiation process in the future.

Conclusion

In conclusion, this study confirmed that DP7-C could efficiently carry miR-26a into cells without cytotoxicity and stimulate cells to secrete exosomes overexpressing miR-26a. Exosomes loaded with miR-26a can be successfully taken up by BMSCs and effectively promote osteogenesis in vitro and *in vivo*. In summary, these findings imply that miR-26a may play an essential role in the osteogenesis of BMSCs via distinct pathways. Exosomes loaded with miR-26a could be a new therapeutic method for repairing bone injury. More mechanistic research is needed to effectively harness these cells for future regenerative therapy.

Declarations

Data availability statement

The datasets used and analyzed during the current study are available from the corresponding author upon reasonable request.

Funding statement

This work was supported by the Department of Science and Technology of Sichuan Province (2021YFS0009) and the Chinese National Natural Science Foundation (82071168).

Conflict of interest disclosure

The authors declare that they have no conflicts of interest.

Ethics approval statement

This study's all animal experiments were done in the animal laboratory center per the study protocol according to the NIH Guide for the Care and Use of Laboratory Animals, approved by the Animal Care and Use Committee of the Sichuan Provincial People's Hospital (Approval No. 20200133).

References

1. Chipashvili, O., & Bor, B. (2022). Ligature-induced periodontitis mouse model protocol for studying Saccharibacteria. *STAR Protoc, 3*(1), 101167. doi:10.1016/j.xpro.2022.101167
2. Dai, Q., Xu, Z., Ma, X., Niu, N., Zhou, S., Xie, F., . . . Zou, W. (2017). mTOR/Raptor signaling is critical for skeletogenesis in mice through the regulation of Runx2 expression. *Cell Death Differ, 24*(11), 1886-1899. doi:10.1038/cdd.2017.110
3. Deng, L., Qing, W., Lai, S., Zheng, J., Liu, C., Huang, H., . . . Mu, Y. (2022). Differential Expression Profiling of microRNAs in Human Placenta-Derived Mesenchymal Stem Cells Cocultured with Grooved Porous Hydroxyapatite Scaffolds. *DNA Cell Biol, 41*(3), 292-304. doi:10.1089/dna.2021.0850

4. Elashiry, M., Elashiry, M. M., Elsayed, R., Rajendran, M., Auersvald, C., Zeitoun, R., . . . Cutler, C. W. (2020). Dendritic cell derived exosomes loaded with immunoregulatory cargo reprogram local immune responses and inhibit degenerative bone disease in vivo. *J Extracell Vesicles, 9*(1), 1795362. doi:10.1080/20013078.2020.1795362
5. Fan, J., Lee, C. S., Kim, S., Chen, C., Aghaloo, T., & Lee, M. (2020). Generation of Small RNA-Modulated Exosome Mimetics for Bone Regeneration. *ACS Nano, 14*(9), 11973-11984. doi:10.1021/acsnano.0c05122
6. Huang, C. C., Kang, M., Lu, Y., Shirazi, S., Diaz, J. I., Cooper, L. F., . . . Ravindran, S. (2020). Functionally engineered extracellular vesicles improve bone regeneration. *Acta Biomater, 109*, 182-194. doi:10.1016/j.actbio.2020.04.017
7. Jin, Z., Ren, J., & Qi, S. (2020). Human bone mesenchymal stem cells-derived exosomes overexpressing microRNA-26a-5p alleviate osteoarthritis via down-regulation of PTGS2. *Int Immunopharmacol, 78*, 105946. doi:10.1016/j.intimp.2019.105946
8. Kalluri, R., & LeBleu, V. S. (2020). The biology, function, and biomedical applications of exosomes. *Science, 367*(6478). doi:10.1126/science.aau6977
9. Lanzillotti, C., De Mattei, M., Mazziotta, C., Taraballi, F., Rotondo, J. C., Tognon, M., & Martini, F. (2021). Long Non-coding RNAs and MicroRNAs Interplay in Osteogenic Differentiation of Mesenchymal Stem Cells. *Frontiers in Cell and Developmental Biology, 9*. doi:ARTN 646032 10.3389/fcell.2021.646032
10. Li, W., Liu, Y., Zhang, P., Tang, Y., Zhou, M., Jiang, W., . . . Zhou, Y. (2018). Tissue-Engineered Bone Immobilized with Human Adipose Stem Cells-Derived Exosomes Promotes Bone Regeneration. *ACS Appl Mater Interfaces, 10*(6), 5240-5254. doi:10.1021/acsami.7b17620
11. Li, Y., Fan, L., Hu, J., Zhang, L., Liao, L., Liu, S., . . . Jin, Y. (2015). MiR-26a Rescues Bone Regeneration Deficiency of Mesenchymal Stem Cells Derived From Osteoporotic Mice. *Mol Ther, 23*(8), 1349-1357. doi:10.1038/mt.2015.101
12. Li, Y., Fan, L., Liu, S., Liu, W., Zhang, H., Zhou, T., . . . Jin, Y. (2013). The promotion of bone regeneration through positive regulation of angiogenic-osteogenic coupling using microRNA-26a. *Biomaterials, 34*(21), 5048-5058. doi:10.1016/j.biomaterials.2013.03.052
13. Li, Z. Y., Li, Q. X., Tong, K., Zhu, J. Y., Wang, H., Chen, B. A., & Chen, L. B. (2022). BMSC-derived exosomes promote tendon-bone healing after anterior cruciate ligament reconstruction by regulating M1/M2 macrophage polarization in rats. *Stem Cell Research & Therapy, 13*(1). doi:ARTN 295 10.1186/s13287-022-02975-0
14. Lian, J. B., Stein, G. S., van Wijnen, A. J., Stein, J. L., Hassan, M. Q., Gaur, T., & Zhang, Y. (2012). MicroRNA control of bone formation and homeostasis. *Nat Rev Endocrinol, 8*(4), 212-227. doi:10.1038/nrendo.2011.234
15. Liu, A., Lin, D., Zhao, H., Chen, L., Cai, B., Lin, K., & Shen, S. G. (2021). Optimized BMSC-derived osteoinductive exosomes immobilized in hierarchical scaffold via lyophilization for bone repair

through Bmpr2/Acvr2b competitive receptor-activated Smad pathway. *Biomaterials, 272*, 120718. doi:10.1016/j.biomaterials.2021.120718

16. Liu, L., Liu, Y., Feng, C., Chang, J., Fu, R., Wu, T., . . . Fang, B. (2019). Lithium-containing biomaterials stimulate bone marrow stromal cell-derived exosomal miR-130a secretion to promote angiogenesis. *Biomaterials, 192*, 523-536. doi:10.1016/j.biomaterials.2018.11.007
17. M.Liu; Y.Sun, Q. Z. (2018). Emerging Role of Extracellular Vesicles in Bone Remodeling. *J Dent Res*.
18. NGF-p75 signaling coordinates skeletal cell migration during bone repair.
19. Peng, B., Chen, Y., & Leong, K. W. (2015). MicroRNA delivery for regenerative medicine. *Adv Drug Deliv Rev, 88*, 108-122. doi:10.1016/j.addr.2015.05.014
20. Pian, C., Zhang, G., Gao, L., Fan, X., & Li, F. (2020). miR+Pathway: the integration and visualization of miRNA and KEGG pathways. *Brief Bioinform, 21*(2), 699-708. doi:10.1093/bib/bby128
21. Roberts, T. C., Langer, R., & Wood, M. J. A. (2020). Advances in oligonucleotide drug delivery. *Nature Reviews Drug Discovery, 19*(10), 673-694. doi:10.1038/s41573-020-0075-7
22. Su, P., Tian, Y., Yang, C., Ma, X., Wang, X., Pei, J., & Qian, A. (2018). Mesenchymal Stem Cell Migration during Bone Formation and Bone Diseases Therapy. *Int J Mol Sci, 19*(8). doi:10.3390/ijms19082343
23. Thakur, A., Parra, D. C., Motallebnejad, P., Brocchi, M., & Chen, H. J. (2022). Exosomes: Small vesicles with big roles in cancer, vaccine development, and therapeutics. *Bioactive Materials, 10*, 281-294. doi:10.1016/j.bioactmat.2021.08.029
24. Vader, P., Mol, E. A., Pasterkamp, G., & Schiffelers, R. M. (2016). Extracellular vesicles for drug delivery. *Adv Drug Deliv Rev, 106*(Pt A), 148-156. doi:10.1016/j.addr.2016.02.006
25. Wang, H., Feng, C., Li, M., Zhang, Z., Liu, J., & Wei, F. (2021). Analysis of lncRNAs-miRNAs-mRNAs networks in periodontal ligament stem cells under mechanical force. *Oral Dis, 27*(2), 325-337. doi:10.1111/odi.13530
26. Xu, X. Y., Tian, B. M., Xia, Y., Xia, Y. L., Li, X., Zhou, H., . . . Chen, F. M. (2020). Exosomes derived from P2X7 receptor gene-modified cells rescue inflammation-compromised periodontal ligament stem cells from dysfunction. *Stem Cells Transl Med, 9*(11), 1414-1430. doi:10.1002/sctm.19-0418
27. Zeng, J. H., Liang, X. Z., Lan, H. H., Zhu, X., & Liang, X. Y. (2018). The biological functions of target genes in pan-cancers and cell lines were predicted by miR-375 microarray data from GEO database and bioinformatics. *Plos One, 13*(10), e0206689. doi:10.1371/journal.pone.0206689
28. Zhai, M., Zhu, Y., Yang, M., & Mao, C. (2020). Human Mesenchymal Stem Cell Derived Exosomes Enhance Cell-Free Bone Regeneration by Altering Their miRNAs Profiles. *Adv Sci (Weinh), 7*(19), 2001334. doi:10.1002/advs.202001334
29. Zhang, R., Tang, L., Tian, Y., Ji, X., Hu, Q., Zhou, B., . . . Yang, L. (2020). DP7-C-modified liposomes enhance immune responses and the antitumor effect of a neoantigen-based mRNA vaccine. *J Control Release, 328*, 210-221. doi:10.1016/j.jconrel.2020.08.023
30. Zhang, R., Tang, L., Zhao, B., Tian, Y., Zhou, B., Mu, Y., & Yang, L. (2021). A Peptide-Based Small RNA Delivery System to Suppress Tumor Growth by Remodeling the Tumor Microenvironment. *Mol*

Pharm, 18(3), 1431-1443. doi:10.1021/acs.molpharmaceut.0c01253

31. Zuo, R., Kong, L., Wang, M., Wang, W., Xu, J., Chai, Y., . . . Kang, Q. (2019). Exosomes derived from human CD34(+) stem cells transfected with miR-26a prevent glucocorticoid-induced osteonecrosis of the femoral head by promoting angiogenesis and osteogenesis. *Stem Cell Research & Therapy, 10*(1), 321. doi:10.1186/s13287-019-1426-3

Figures

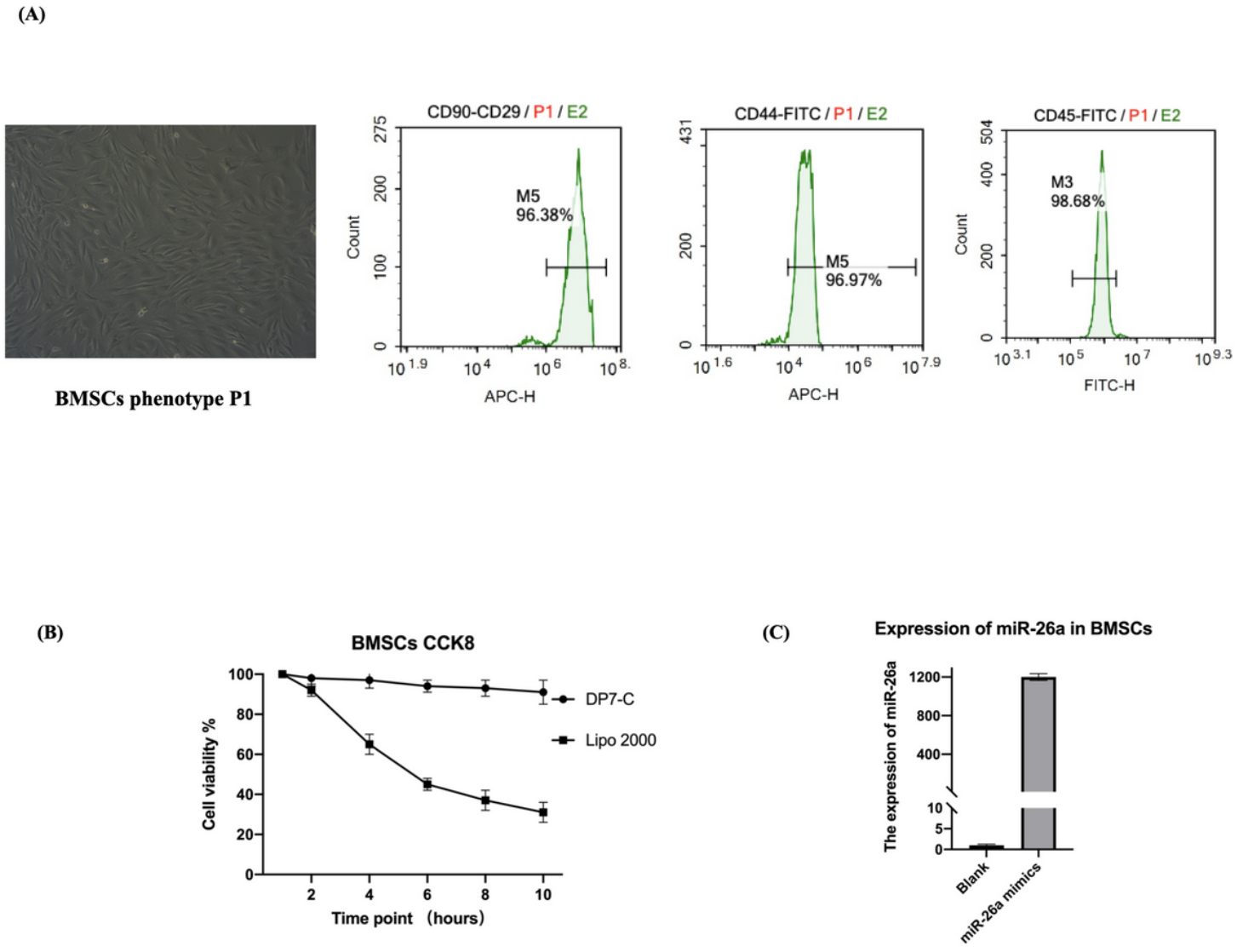

Figure 1

The efficiency of DP7-C-transfected miRNA-26a and toxicity assessment.

A. Morphological characterization of P1 BMSCs.

B. Detection of the cytotoxicity of DP7-C and Lipo2000 by CCK-8 assay.

C. The efficiency of DP7-C transfection of miR-26a in BMSCs measured by qRT—PCR. For normalization, U6 was utilized.

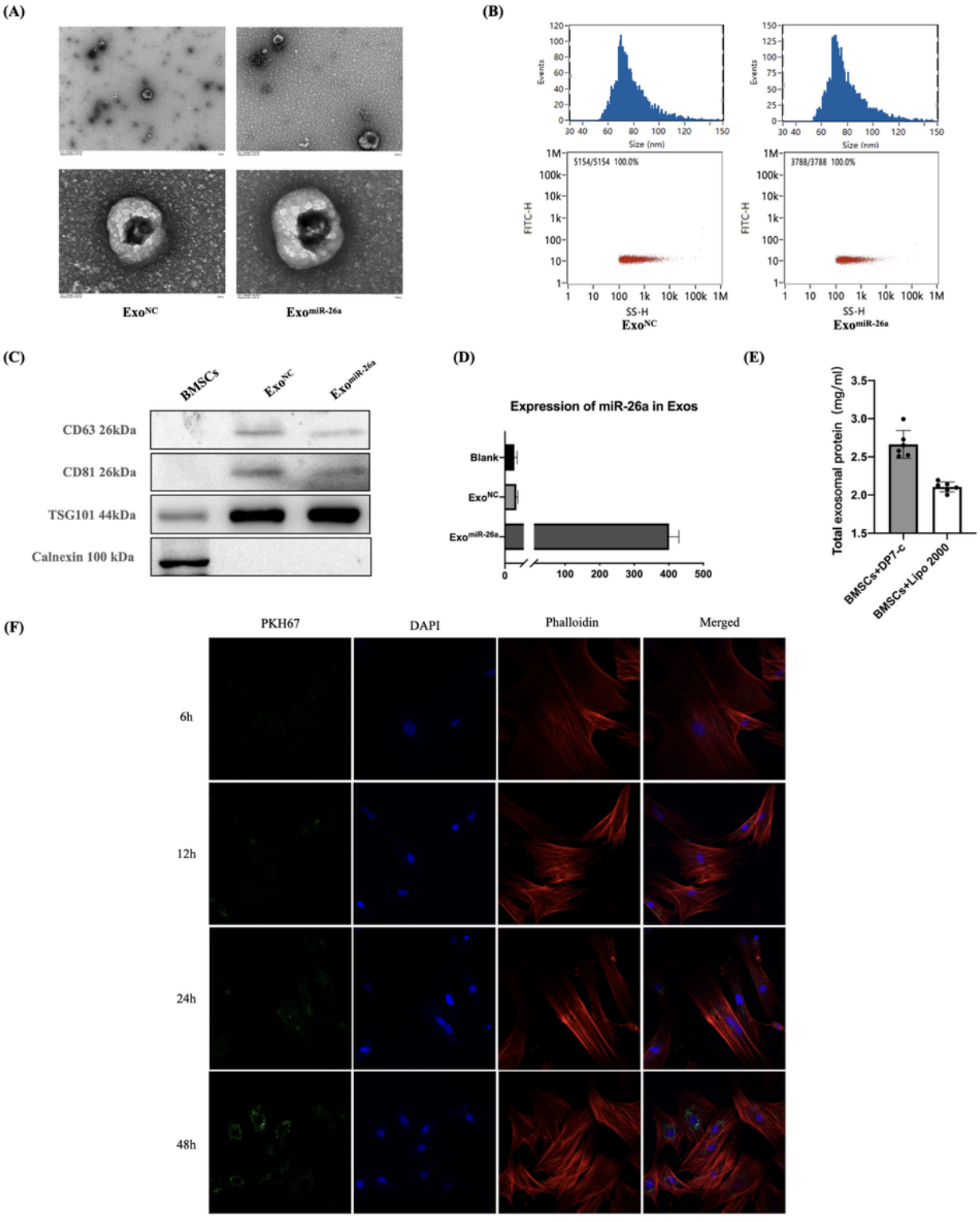

Figure 2

Identification of exosomes.

A. Transmission electron microscopy (TEM) to visualize the shape of exosomes.

B. Nanoparticle tracking analysis (NTA) to analyze particle size.

C. Western blotting to detect Exo-related protein markers, including CD63, CD81, Tsg101, and the negative marker Calnexin.

D. The expression of miR-26a in Exos secreted from modified BMSCs. For normalization, U6 was utilized.

E. Concentrations of exosomal proteins with different transfection reagents. Exosomes were isolated from 116.1 ml of supernatant and resuspended in 60 μl of lysis buffer.

F. BMSCs gradually took up PKH67-labeled exosomes (green) at 6, 24, and 48 hours. The nuclei of BMSCs were stained with DAPI (blue), and the cytoskeleton was labeled with phalloidin (red).

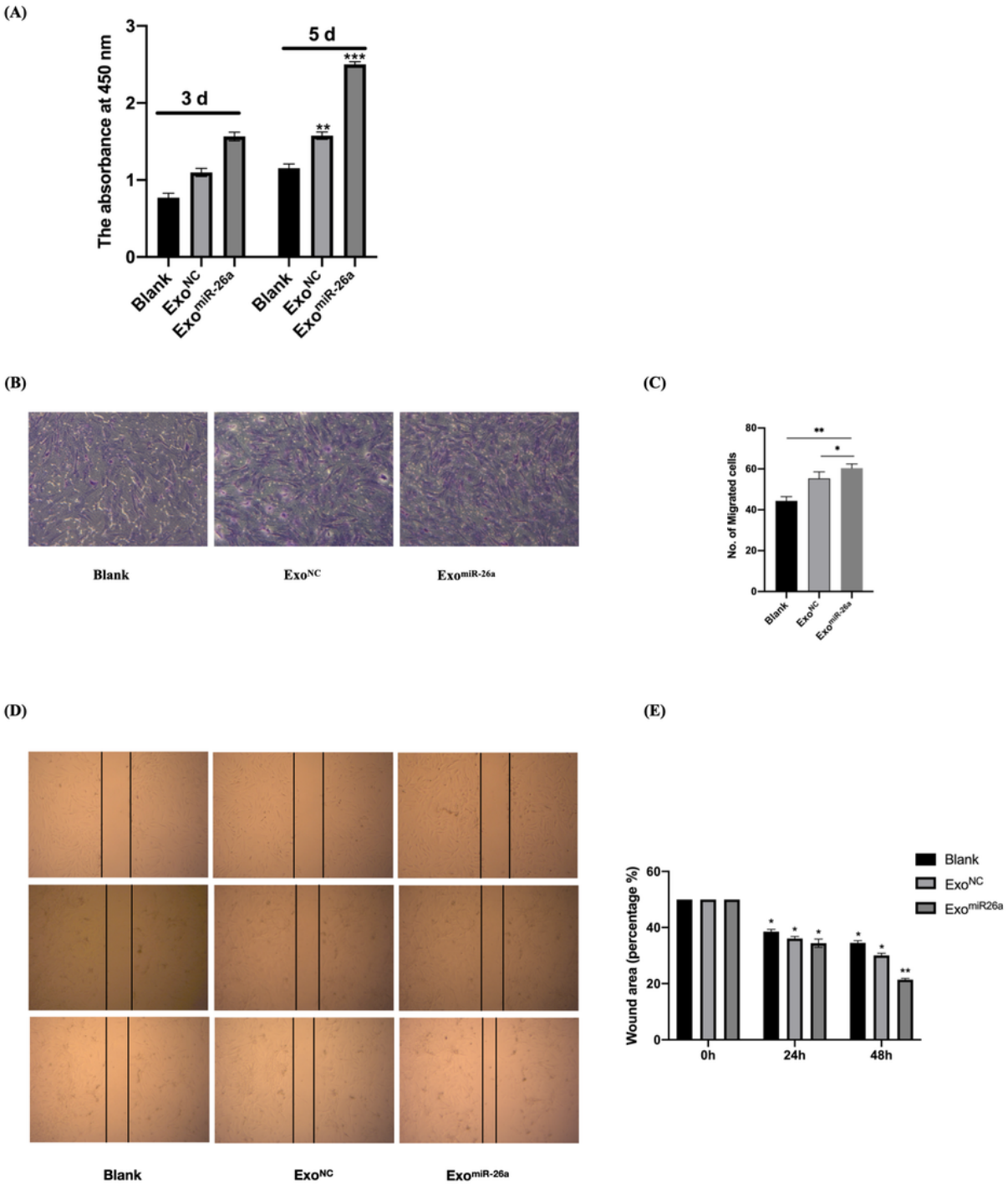

Figure 3

Exos loaded with miR-26a promoted the proliferation and migration of BMSCs.

A. The effect of exosomes on cell proliferation was assessed by CCK-8 assay.

B-C. Transwell assay to evaluate the function of exosomes loaded with miR-26a in cell migration.

D-E. Migration of BMSCs cocultured with exosomes and columnar analysis diagram.

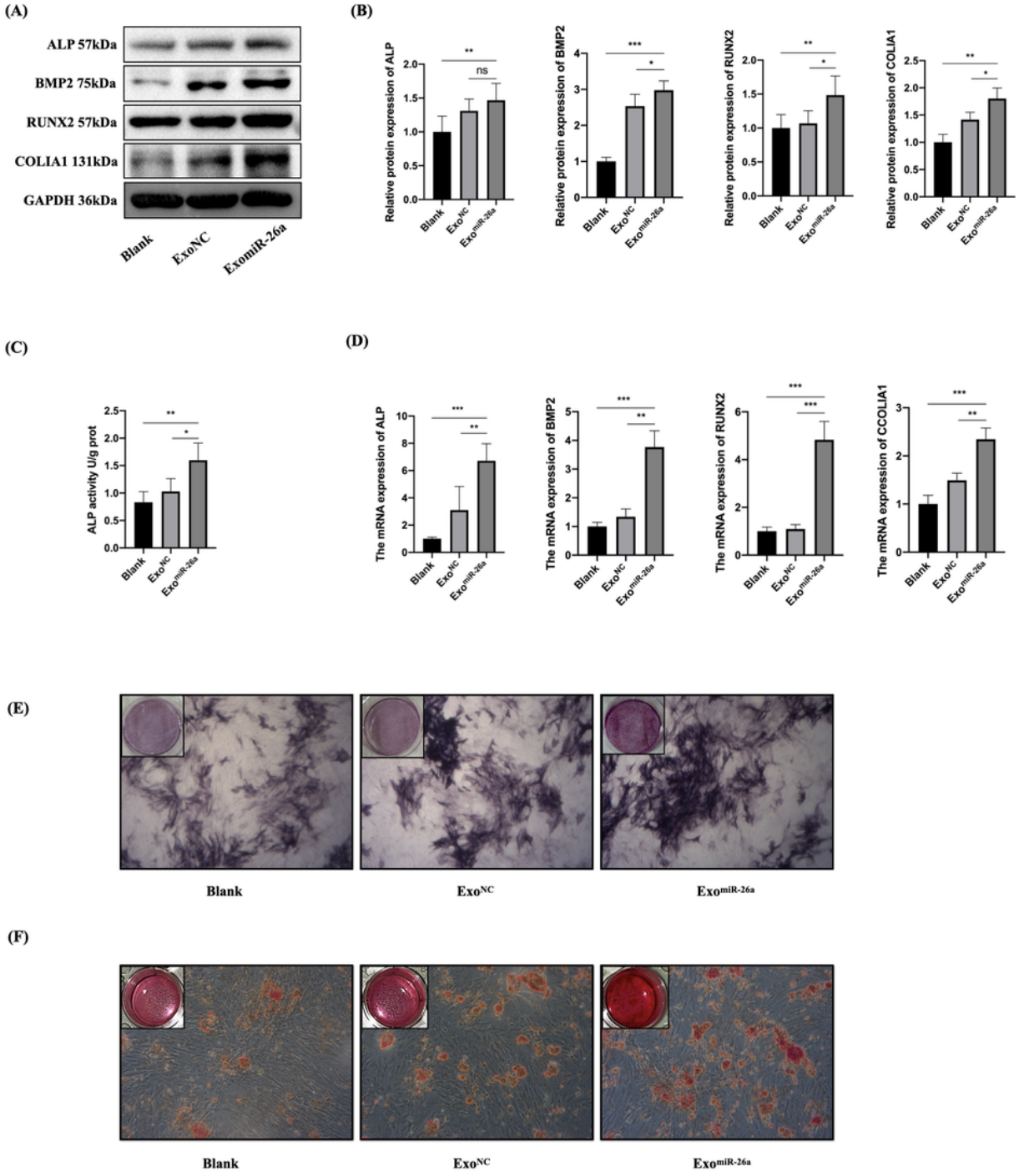

Figure 4

Exos loaded with miR-26a promote osteogenic differentiation of BMSCs

A-B. The expression of the osteogenesis-related proteins ALP, BMP2, Runx2, and COLIA 1 was detected by western blotting. Protein quantification by ImageJ.

C. ALP activity detection after osteogenic induction for 7 days.

D. Relative mRNA expression of the osteogenesis-related genes ALP, BMP2, Runx2, and COLIA 1 measured by qRT—PCR. GAPDH was utilized for normalization. For three separate trials, data are represented as the mean ± SD. * indicates $P < 0.05$; ** indicates $P < 0.01$; NS indicates not significant.

ALP, alkaline phosphatase; BMP2, bone morphogenetic protein 2; RUNX2, runt-related transcription factor 2; COLIa1, collagen type I alpha 1; GAPDH, glyceraldehyde-3-phosphate dehydrogenase.

E. ALP staining after osteogenic induction for 7 days.

F. Alizarin red S staining after osteogenic induction for 14 days.

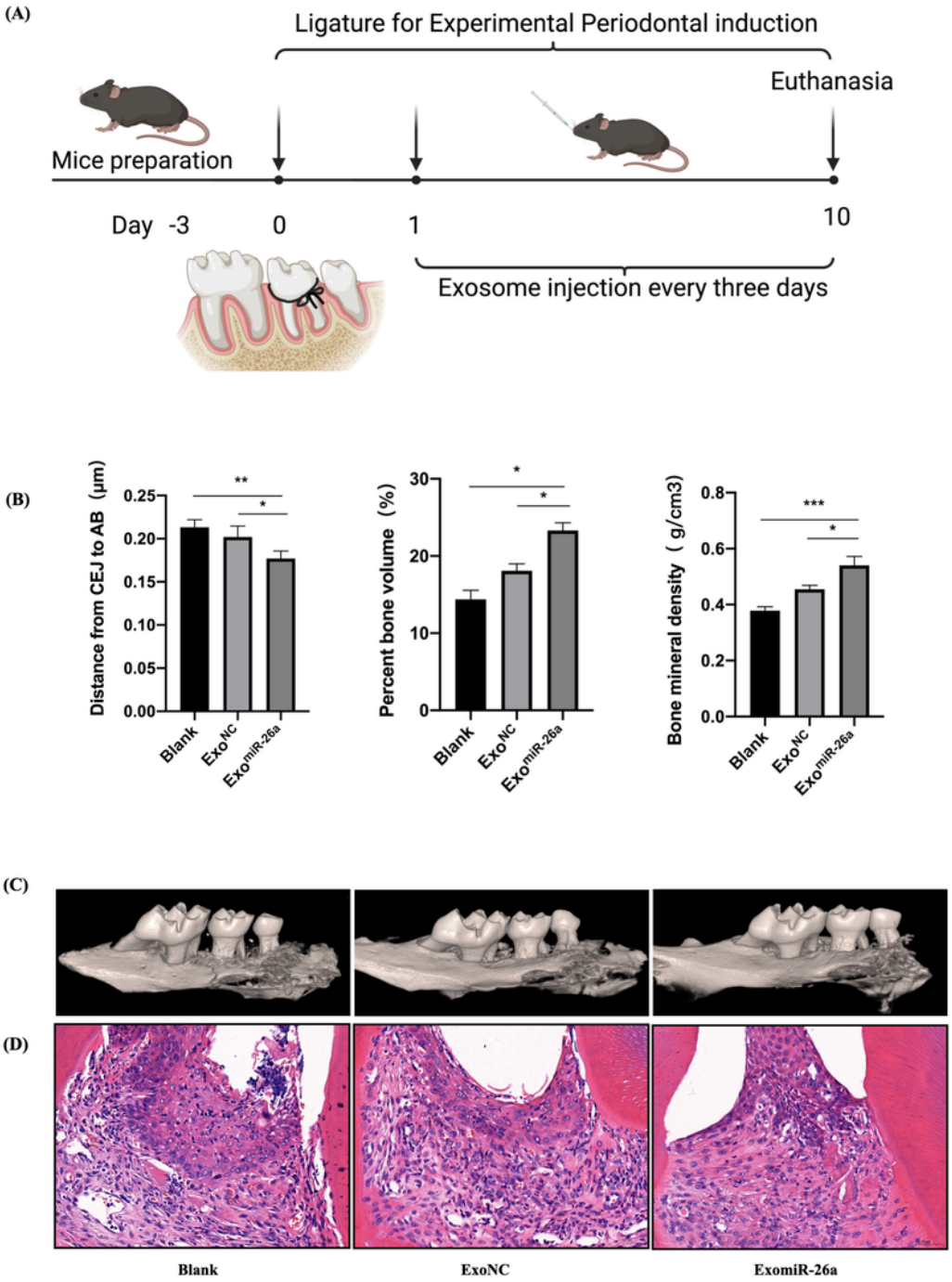

Figure 5

The effects of Exos loaded with miR-26a *in vivo*.

A. Schematic diagram of the animal experiments in this study.

B. Quantification of bone regeneration included the distance from the CEJ to the AB, percentage of bone volume (BV/TV, bone volume/tissue volume), and bone mineral density (BMD).

C. Representative three-dimensional reconstruction images of the upper right maxilla.

D. Hematoxylin-eosin staining of the periodontal tissue.

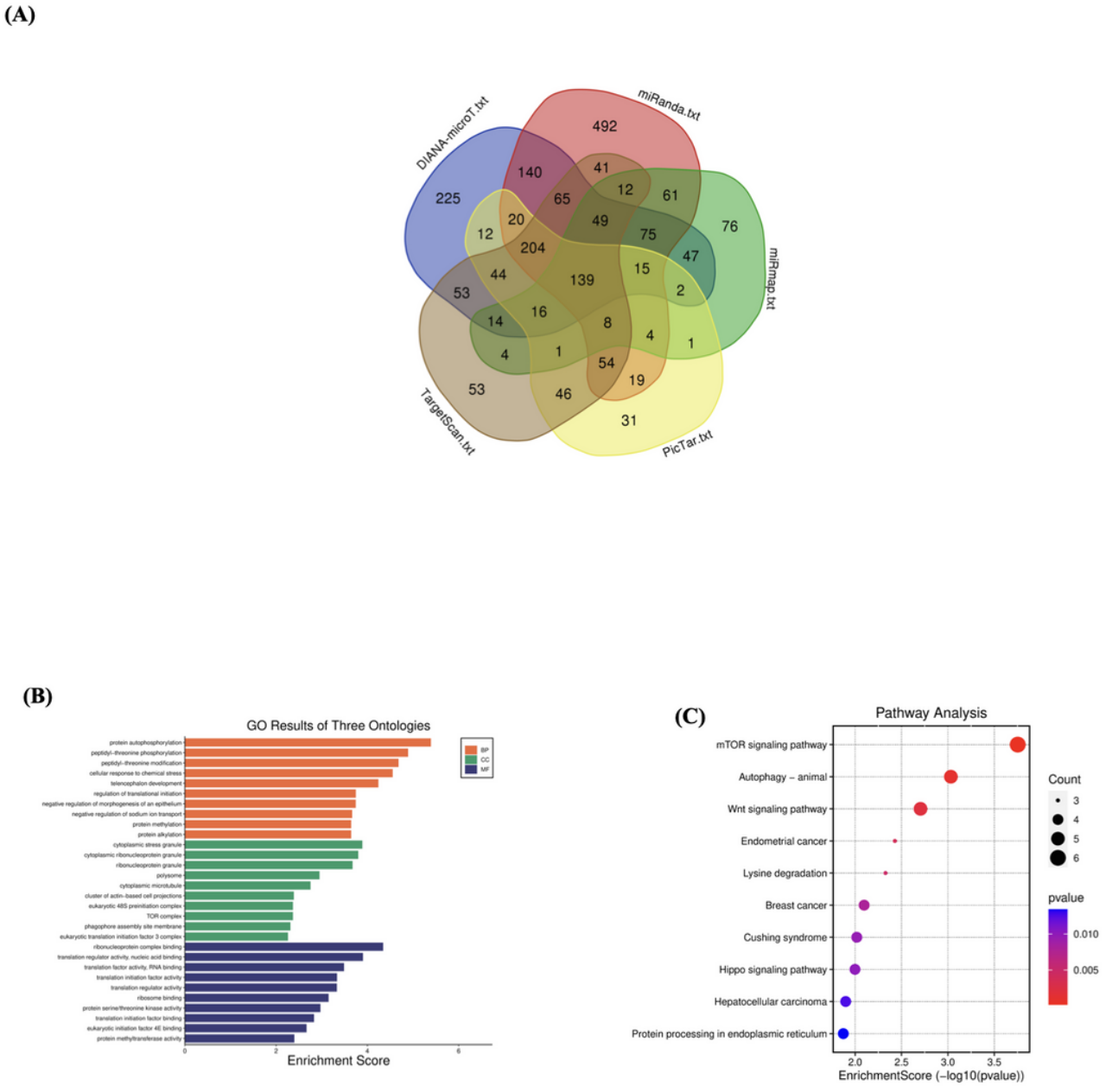

Figure 6

Identifying promising miR-26a target genes in BMSC osteogenesis using bioinformatics.

A. The junction of the predicted target genes presented by veen.

B. The enrichment map from Gene Ontology (GO) analysis, including biological process (BP), cellular component (CC), and molecular function (MF).

C. KEGG (Kyoto Encyclopedia of Genes and Genomes) pathway analysis of gene targets of miR-26a in BMSCs.